NOAA Technical Memorandum NWS NMC 66

THE LFM-II MODEL -- 1980

Washington, D.C.
September 1981

U.S. DEPARTMENT OF COMMERCE / National Oceanic and Atmospheric Administration / National Weather Service

National Meteorological Center
National Weather Service, National Meterological Center Series

The National Meteorological Center (NMC) of the National Weather Service (NWS) produces weather analyses and forecasts for the Northern Hemisphere. Areal coverage is being expanded to include the entire globe. The Center conducts research and development to improve the accuracy of forecasts, to provide information in the most useful form, and to present data as automatically as practicable.

NOAA Technical Memorandums in the NWS NMC series facilitate rapid dissemination of material of general interest which may be preliminary in nature and which may be published formally elsewhere at a later date. Publications 34 through 37 are in the former series, Weather Bureau Technical Notes (TN), National Meterological Center Technical Memoranda; publications 38 through 48 are in the former series ESSA Technical Memoranda, Weather Bureau Technical Memoranda (WBTM). Beginning with 49, publications are now part of the series, NOAA Technical Memorandums NWS.

Publications listed below are available from the National Technical Information Service (NTIS), U.S. Department of Commerce, Sills Bldg., 5285 Port Royal Road, Springfield, VA 22161. Prices vary for paper copies; $3.50 microfiche. Order by accession number, when given, in parentheses.

Weather Bureau Technical Notes

TN 22 NMC 34 Tropospheric Heating and Cooling for Selected Days and Locations over the United States During Winter 1960 and Spring 1962. Philip F. Clapp and Francis J. Winninghoff, 1965, 18 pp. (PB-170-584)

TN 30 NMC 35 Saturation Thickness Tables for the Dry Adiabatic, Pseudo-adiabatic, and Standard Atmospheres. Jerrold A. LaRue and Russell J. Younkin, January 1966, 18 pp. (PB-169-382)

TN 37 NMC 36 Summary of Verification of Numerical Operational Tropical Cyclone Forecast Tracks for 1965. March 1966, 6 pp. (PB-170-410)

TN 40 NMC 37 Catalog of 5-Day Mean 700-mb. Height Anomaly Centers 1947-1963 and Suggested Applications. J. F. O'Connor, April 1966, 63 pp. (PB-170-376)

ESSA Technical Memoranda

WBTM NMC 38 A Summary of the First-Guess Fields Used for Operational Analyses. J. E. McDonell, February 1967, 17 pp. (AD-810-279)

WBTM NMC 39 Objective Numerical Prediction Out to Six Days Using the Primitive Equation Model--A Test Case. A. J. Wagner, May 1967, 19 pp. (PB-174-920)

WBTM NMC 40 A Snow Index. R. J. Younkin, June 1967, 7 pp. (PB-175-641)

WBTM NMC 41 Detailed Sounding Analysis and Computer Forecasts of the Lifted Index. John D. Stackpole, August 1967, 8 pp. (PB-175-928)

WBTM NMC 42 On Analysis and Initialization for the Primitive Forecast Equations. Takashi Nitta and John B. Hovermale, October 1967, 24 pp. (PB-176-510)

WBTM NMC 43 The Air Pollution Potential Forecast Program. John D. Stackpole, November 1967, 8 pp. (PB-176-949)

WBTM NMC 44 Northern Hemisphere Cloud Cover for Selected Late Fall Seasons Using TIROS Nephanalyses. Philip F. Clapp, December 1968, 11 pp. (PB-186-392)

WBTM NMC 45 On a Certain Type of Integration Error in Numerical Weather Prediction Models. Hans Okland, September 1969, 23 pp. (PB-187-795)

WBTM NMC 46 Noise Analysis of a Limited-Area Fine-Mesh Prediction Model. Joseph P. Gerrity, Jr., and Ronald D. McPherson, February 1970, 81 pp. (PB-191-188)

WBTM NMC 47 The National Air Pollution Potential Forecast Program. Edward Gross, May 1970, 28 pp. (PB-192-324)

WBTM NMC 48 Recent Studies of Computational Stability. Joseph P. Gerrity, Jr., and Ronald D. McPherson, May 1970, 24 pp. (PB-192-979)

(Continued on inside back cover)

NOAA Technical Memorandum NWS NMC 66

THE LFM-II MODEL -- 1980

John E. Newell and
Dennis G. Deaven

Washington, D.C.
September 1981

UNITED STATES
DEPARTMENT OF COMMERCE
Malcolm Baldrige, Secretary

National Oceanic and
Atmospheric Administration
John V. Byrne, Administrator

National Weather
Service
Richard E. Hallgren, Director

CONTENTS

THE LFM-II MODEL -- 1980

John E. Newell and Dennis G. Deaven

NOAA, NWS, National Meteorological Center
Washington, DC 20233

ABSTRACT. The changes incorporated in the LFM model since the end of 1976 are documented. Emphasis is placed on the computational grids used by the model and on its vertical structure. The calculation of convective precipitation and the vertical interpolation from the model's coordinate to isobaric surfaces for display purposes are treated in detail. The circulation and precipitation forecasts of the LFM are evaluated by presenting monthly values of S1 scores and of threat scores for the years 1976 through 1979.

1. INTRODUCTION

The purpose of this NOAA Technical Memorandum is to bring up to date the information contained in the previous documentation of the LFM model by Gerrity (1977). The description in that work was current as of the end of 1976. Since then, some important changes have been made in the procedures used in the limited area forecast system.

The previous documentation was quite detailed and the bulk of it is still valid. There is, therefore, no need to repeat it here. Instead, we will focus either on features of the model which were not described by Gerrity (1977) or on those aspects of the June 1980 version of the LFM which differ from the model as it was at the end of 1976.

2. THE GRIDS USED BY THE MODEL

The LFM forecast is computed on a polar stereographic map projection true at 60 degrees north latitude. Two distinct grids, covering exactly the same geographical area of the globe, are used by the model. The first of these is the LFM-I grid, an array consisting of 53 columns along the I-axis and 45 rows along the J-axis for a total of 2385 grid-points. The second grid is the LFM-II grid in which I ranges from 1 to 79 and J from 1 to 67, a total of 5293 points.

The grid spacing of the LFM-I grid is 190.5 km at 60 degrees north latitude, while that of the LFM-II is exactly two thirds of this value, or 127.0 km. Essentially, each two grid intervals of LFM-I are replaced by three of LFM-II. The coordinates of the two grids are related by the formulas

$$I_2 = \frac{3}{2}(I_1 - 1) + 1 \qquad (2.1)$$

$$J_2 = \frac{3}{2} (J_1 - 1) + 1 \qquad (2.2)$$

The analyses prepared for the LFM model are contained on the LFM-I grid. When they are read into the computer by the model initialization code, they are immediately interpolated biquadratically to the LFM-II grid so that the initialization process itself is carried out on the finer mesh grid, as is the complete forecast calculation. The post-processing section of the LFM model, which prepares the calculation for display at six-hour intervals, is performed on the LFM-II grid. As a final step, those fields selected for display are interpolated to the LFM-I grid for processing by graphics and other output programs.

The rationale for having the analyses and the display on the LFM-I grid is flexibility and economy of programming. The motivation for computing the initialization and the forecast on the LFM-II grid is to gain the greatest possible accuracy within the limits imposed by the available resources.

3. THE PRESSURE GRADIENT AVERAGING TECHNIQUE

When the LFM-I was converted to LFM-II, it was not necessary to reduce the time step despite the reduction in mesh length. This is so because of the introduction of an economical time integration scheme which has been discussed by Shuman (1971) and by Brown and Campana (1978).

The essential feature of this method is that the pressure gradient term is not evaluated at a single time level, but rather is represented by a time-averaged value. If we let ϕ_x denote the pressure gradient term in the tendency equation for the u-component of the wind, then ϕ_x is evaluated as

$$\phi_x = \alpha \, (\phi_x^{\tau+1} + \phi_x^{\tau-1}) + (1 - 2\alpha) \, \phi_x^{\tau} \qquad (3.1)$$

with a similar expression for ϕ_y. Here τ denotes the time level at which the quantity is to be evaluated and α is a real number.

Use of pressure gradient averaging allows for a timestep increment up to twice as large as that used in the conventional leapfrog time-differencing scheme. However, in order to control computational modes which amplify as powers of the time, the model employs time-smoothing of the predicted quantities. The use of the time damping results in a reduction of the maximum allowable time increment to a value somewhat less than twice that of the usual leapfrog scheme.

The time smoothing of a forecast variable, u for example, can be written as

$$u^{\tau} = b \, (u_*^{\tau+1} + u^{\tau-1}) + (1 - 2b) \, u_*^{\tau} \qquad (3.2)$$

where the asterisk subscript refers to an intermediate value and the absence of it refers to the time-smoothed value. The quantity b is a damping coefficient. As shown by Brown and Campana (1978), for a given choice of b, there is a value of α in equation (3.1), which affords the maximum stable time step. This optimum value of α, namely α_{MAX}, is related to the time filter coefficient by

$$\alpha_{MAX} = (b^2 + 1)\ (b + 1)/4 \tag{3.3}$$

In the current LFM-II, b is given a value of 0.075 and α is computed from equation (3.3).

4. THE VERTICAL STRUCTURE OF THE LFM

The model is divided into three distinct domains in the vertical. These are the boundary layer, the tropospheric and the stratospheric domains. The vertical coordinate used in the model is a modification of the sigma system of Phillips (1957). Sigma is a dimensionless number defined as the ratio of two pressures.

In the boundary layer domain, sigma is given by

$$\sigma_B = \frac{p - (p_G - p_B)}{p_B} \tag{4.1}$$

where p is the pressure at some level in the boundary layer, p_G is the pressure at the ground and p_B is a constant (50 mb) representing the fixed depth of the boundary layer.

In the tropospheric domain, sigma is written as

$$\sigma_T = \frac{p - p_T}{p_G - p_B - p_T} \tag{4.2}$$

where p is an arbitrary pressure level in the troposphere and p_T is the tropopause pressure.

In the stratospheric domain, sigma is defined by

$$\sigma_S = \frac{p - p_{50}}{p_T - p_{50}} \tag{4.3}$$

where p is an arbitrary pressure level in the stratosphere and p_{50} represents the constant value of the 50 mb isobaric surface, which is taken as the top of the model.

Note that in each domain σ varies from a value of 0 at the top (lower pressure) to a value of 1 at the bottom (higher pressure). The stratosphere is divided into three layers, each of pressure thickness equal to $(p_T - p_{50})/3$. The troposphere is also divided into three layers, each of pressure thickness $(p_G - p_B - p_T)/3$. With the addition of the boundary layer, the model is appropriately termed the 7-layer LFM. Wind and temperature are predicted in each of the layers, while precipitable water is forecast in the three lowest layers.

The ground surface, the tropopause and the 50 mb level are considered to be material surfaces, with the result that the vertical velocity, $\dot{\sigma}$, vanishes at those levels. Elsewhere, $\dot{\sigma}$ is computed diagnostically at the interface between each of the model layers.

The vertical structure of the model is indicated in Figure 1. The solid lines are called sigma levels or sigma surfaces and mark the upper and lower boundaries of the layers. The dashed lines represent the midpoint of the layers. The predicted values of wind component, u and v, potential temperature, θ, and moisture, RH, are considered to be carried in the middle of the layers. The height, Z, and vertical velocity, $\dot{\sigma}$, are computed diagnostically and are located at the sigma levels.

5. CALCULATION OF CONVECTIVE PRECIPITATION

Because moisture is carried in only three layers of the present version of the LFM model, the scheme for the parameterization of convection can only crudely approximate atmospheric convective processes. The algorithm is applied layer by layer, starting in the boundary layer and working upward at each column of grid points. Convective precipitation is computed once an hour (every ninth timestep) in order to conserve computer resources.

The algorithm is presented in the flow chart following this section, in which the index k refers to the model layer under consideration. As shown in the flow diagram, there are four tests applied to the layer to determine the occurrence of convection. These are:

1. The mean relative humidity in the layer must be at least 75 percent.

2. There must be convergence of precipitable water, W, into the layer as measured by a positive tendency in W.

3. The pressure of the lifting condensation level of a parcel originating at the midpoint of layer k must be greater than the pressure at the midpoint of layer (k + 1).

4. When lifted to the midpoint of layer (k + 1), the parcel must be warmer than its environment.

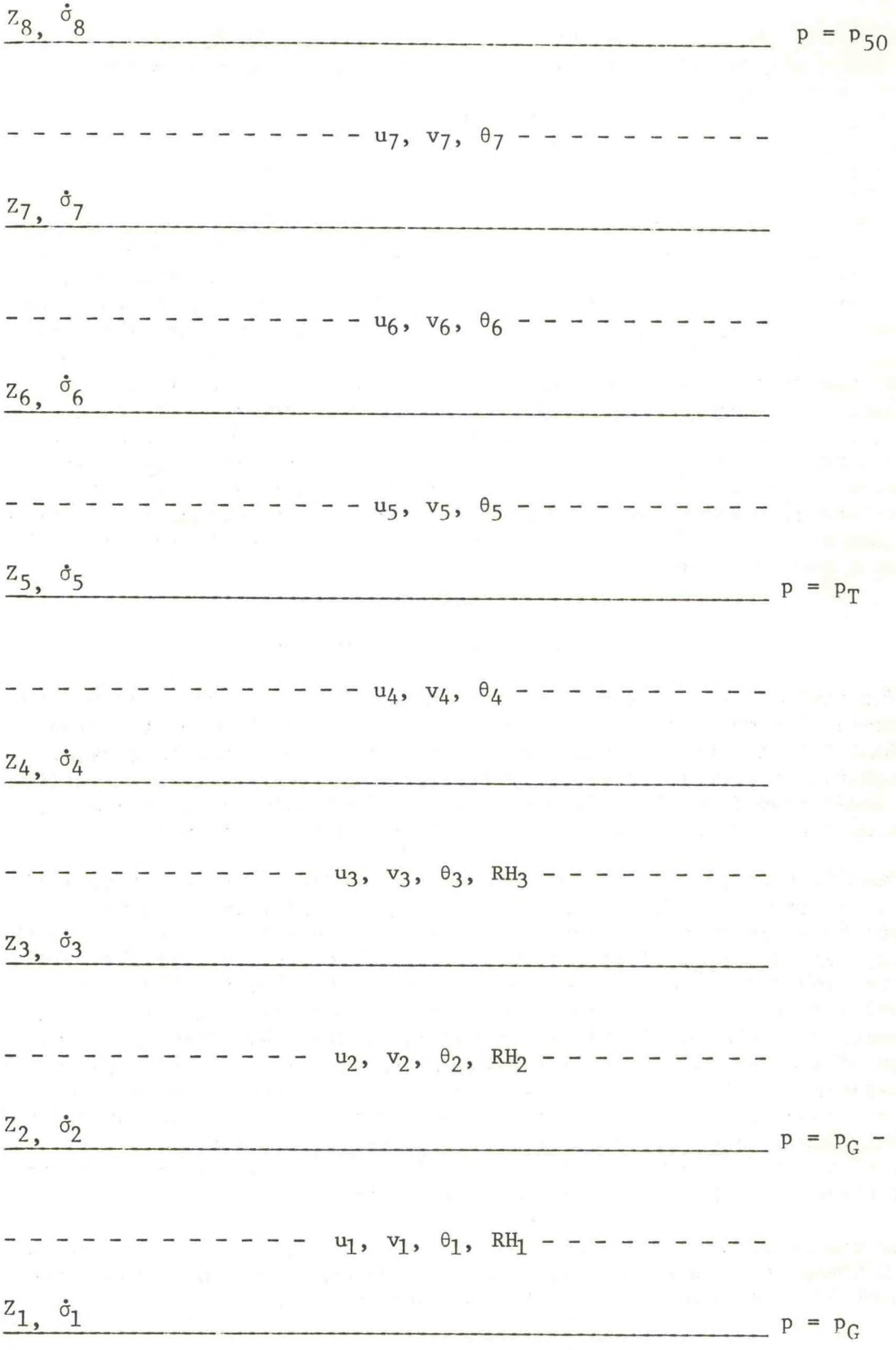

Figure 1. Vertical Structure of the LFM-II Model.

When all the conditions for convection are satisfied, an amount of precipitation attributed to convection is computed from the formula

$$\text{CNRAIN} = \frac{\Delta\theta \; c_p \; \Delta \; p_{k+1} \; \overline{\Pi}_{k+1}}{gL} \tag{5.1}$$

where $\Delta\theta$ is the difference between the temperature of the parcel lifted, first dry and then moist adiabatically, to the midpoint of layer (k + 1) and the temperature of the environment at that level, c_p is the specific heat of dry air at constant pressure, ΔP_{k+1} is the pressure thickness of layer (k + 1), $\overline{\Pi}_{k+1}$ is the value of the Exner function at the midpoint of layer (k + 1), g is the acceleration of gravity and L is the latent heat of vaporization or condensation. The precipitable water in layer k is reduced by an amount equal to CNRAIN. In addition, the potential temperature of layer (k + 1) is increased by an amount $\Delta\theta$. This aspect of the scheme was designed to simulate convective pumping of heat aloft in cumulus clouds. Also, it should be noted in the flow chart that the temperature of layer k is increased by 2 degrees Kelvin prior to computing the pressure of the LCL. This is done to simulate large scale lifting by enhancing the buoyancy.

6. LATERAL BOUNDARY CONDITIONS

The five outermost grid rows surrounding the LFM forecast area form the lateral boundary region. Values for the specification of the time-dependent lateral boundaries of the LFM are obtained from a large-scale (hemispheric or global) forecast made twelve hours earlier. The large-scale prediction from 12 to 60 hours, at six-hour intervals, is used to determine large-scale tendencies at the boundary zone grid points.

The first step in this procedure is the horizontal interpolation of forecast isobaric fields of wind, height, temperature, and tropopause pressure from the grid points of the large-scale model to those of the LFM boundary region. A vertical interpolation is then done at the LFM points from the isobaric values to the sigma system of the 7-layer LFM. The vertical interpolation uses the same techniques employed in the initialization section of the model and yields values of wind and potential temperature in each of the layers, and of the pressure thickness of the troposphere and stratosphere. Next, the sigma layer values are time-differenced to form six-hour tendencies, which are then scaled to the timestep used by the LFM. Finally, large-scale values of wind, temperature, and pressure thickness at points of the boundary region are obtained at each timestep by adding the scaled tendency to the LFM model's initial values.

At the outermost row of grid points, these large-scale values are used at each timestep without modification. At the next four inner rows (rows 2 through 5) a diffusive "nudge" in the form of:

$$\phi_{LFM}^{\tau+1} = \phi_{LFM}^{\tau-1} + 2\,\Delta t\left(\frac{\partial \phi_{LFM}^{\tau}}{\partial t}\right) + K\,\nabla^2\,(\phi_{LFM}^{\tau-1} - \phi_{LS}^{\tau-1}) \tag{6.1}$$

Convective Precipitation Flow Chart

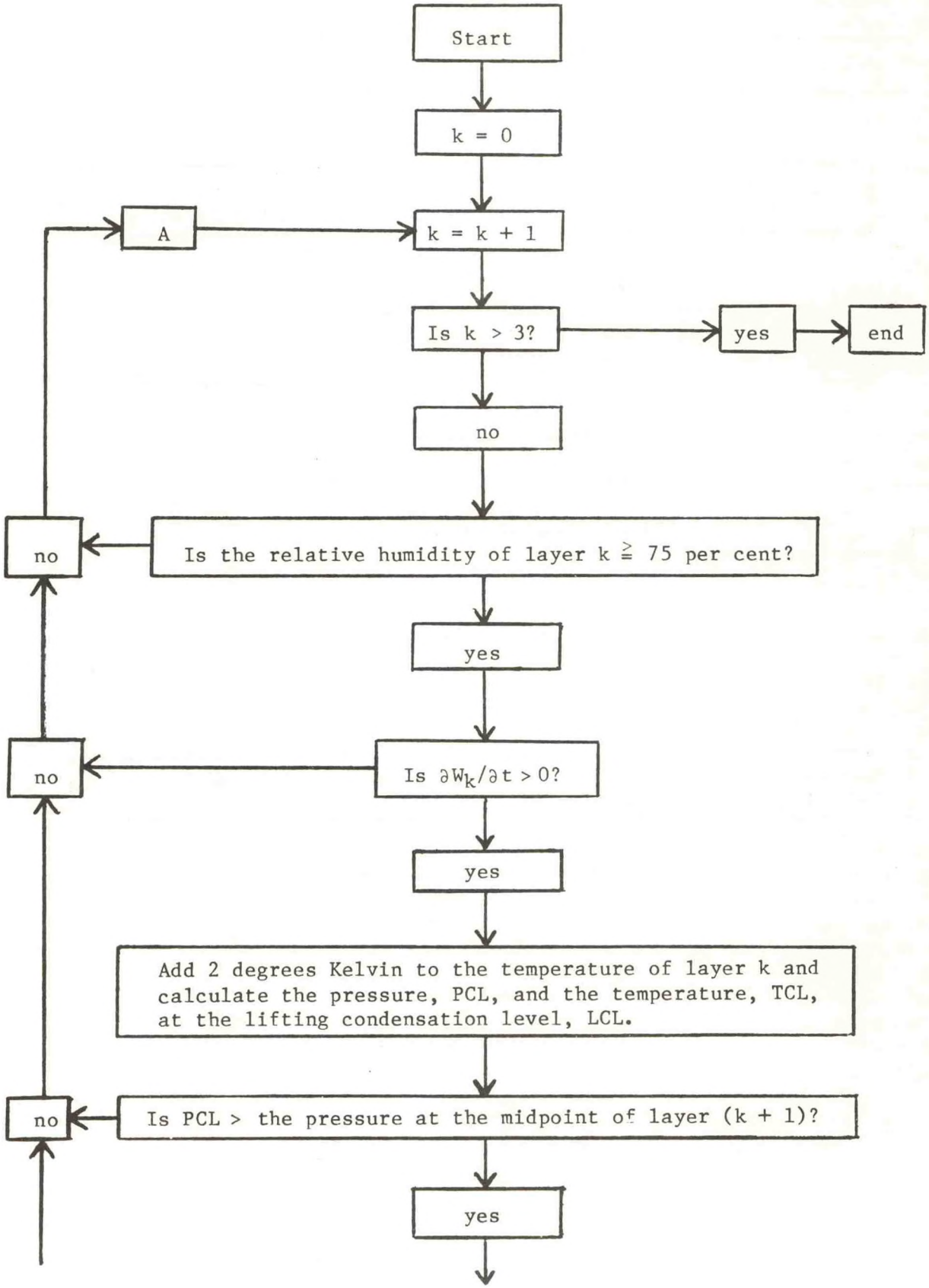

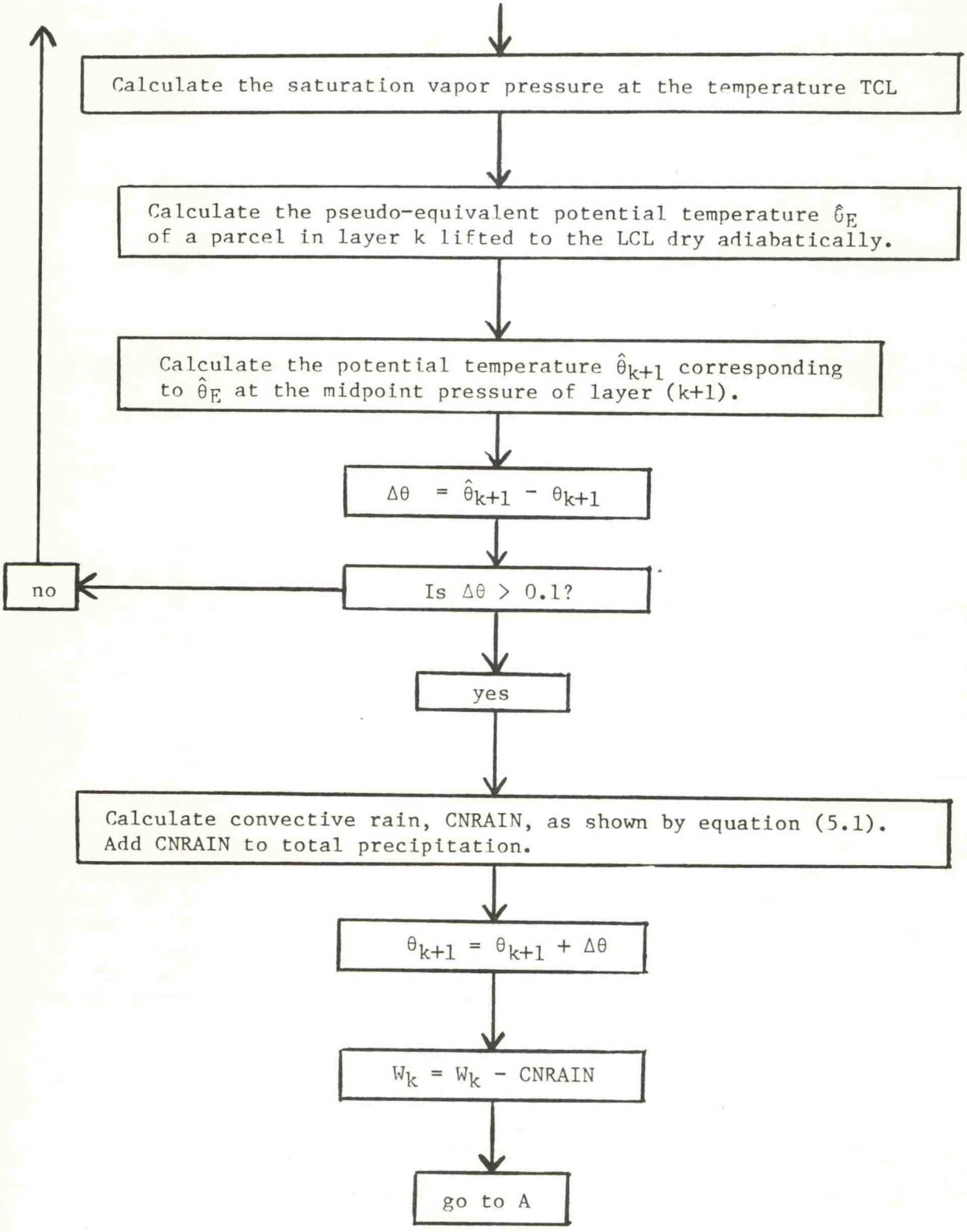
Calculate the saturation vapor pressure at the temperature TCL
Calculate the pseudo-equivalent potential temperature $\hat{\theta}_E$ of a parcel in layer k lifted to the LCL dry adiabatically.
Calculate the potential temperature $\hat{\theta}_{k+1}$ corresponding to $\hat{\theta}_E$ at the midpoint pressure of layer (k+1).
$\Delta\theta = \hat{\theta}_{k+1} - \theta_{k+1}$
Is $\Delta\theta > 0.1$?
no
yes
Calculate convective rain, CNRAIN, as shown by equation (5.1). Add CNRAIN to total precipitation.
$\theta_{k+1} = \theta_{k+1} + \Delta\theta$
$W_k = W_k - CNRAIN$
go to A

is used to modify the LFM grid point values. Here ϕ represents a prognostic variable, the superscript τ denotes the timestep index, the subscript LFM denotes a value obtained from the model equations and the subscript LS refers to the large-scale value.

The finite form of the Laplacian operator is defined by:

$$\nabla^2\phi_{I,J} = \phi_{I+1,J} + \phi_{I-1,J} + \phi_{I,J+1} + \phi_{I,J-1} - 4\phi_{I,J} \qquad (6.2)$$

and the value of the diffusion coefficient, K, is fixed at 0.04 in the boundary region. Note that all space and time scales have been absorbed in the value of K and the finite form of the Laplacian. This procedure is applied during each timestep of the model's integration to all prognostic variables except precipitable water which is kept constant on the boundary.

If a large-scale forecast is not available, then LFM grid points on the outermost row are kept fixed at their initial values during the integration and the contribution of the large-scale model to the Laplacian in Equation (6.1) is set equal to zero. This procedure produces a constant boundary condition with increased diffusion in the boundary zone.

7.1 Post-Processing the Forecast

At six-hour intervals after initial time the forecast calculations are interpolated vertically from the sigma-coordinate system to standard isobaric levels and then are filtered horizontally for display and transmission to users. This procedure is known as post-processing and its principal steps will be described in the next three sections.

7.2 The Vertical Interpolation from Sigma to Pressure

The pressure at each of the sigma levels shown in Figure 1 is obtained by using the forecast values of pressure thickness in the stratospheric and tropospheric domains and integrating downward from the top of the model at 50 mb to the earth's surface. Values of the Exner function and of the logarithm of pressure are computed from the pressure at the sigma levels. A value of the Exner function in the middle of each layer is calculated from the values on the sigma levels, and from this a value of the logarithm of pressure in the middle of the layer is determined.

The absolute temperature, T, at sigma levels other than the tropopause is defined by modeling T linear in logarithm of pressure. The height, Z, of each sigma surface is computed by integrating upward from the ground, using the forecast pressure-temperature profile in the vertical.

Temperature, T, at the tropopause is obtained as a weighted mean of a value, T_A, extrapolated from above the tropopause, and a value, T_B, extrapolated from below. The extrapolation is done by modeling T linear in pressure. Using the vertical indexing scheme shown in Figure 1, T_A and T_B can be written as:

$$T_A = 1.5\ T_5 - 0.5\ T_6$$
$$T_B = 1.5\ T_4 - 0.5\ T_3 \qquad (7.1)$$

It is convenient to define some additional quantities.

$$a \equiv (p_T - p_{50})/3$$
$$b \equiv (P_G - p_B - p_T)/3 \qquad (7.2)$$
$$\alpha \equiv \frac{2a}{a + b}$$
$$\beta \equiv \frac{2b}{a + b}$$

The value of tropopause temperature, T*, is computed as

$$T^* = (\alpha\ T_B + \beta\ T_A)/2 \qquad (7.3)$$

The wind components (u*, v*) at the tropopause level are computed using the same procedure employed for temperature.

Temperature, wind, and relative humidity at standard isobaric levels are computed using the values in the sigma layers. It is assumed that each of these quantities varies linearly in the log of pressure.

For isobaric levels located above ground, the height is computed hydrostatically from the values of height on the sigma surfaces and the known vertical distribution of temperature. T is modeled linear in log of pressure.

At gridpoints where a desired isobaric level lies below the ground, the height of that level is computed using a technique designed to simulate, at least in part, the method employed at observing stations to reduce the measured station pressure to a value of sea-level pressure. Using the symbols of Figure 1 we define

$$\overline{Z}_2 \equiv 0.5\ (Z_2 + Z_3)$$
$$T_* \equiv T_2 - 0.0065\ (Z_1 - \overline{Z}_2) \qquad (7.4)$$
$$T_{SL} \equiv T_* + 0.0065\ Z_1$$

If T_{SL} is less than or equal to 290.66K, the height of the isobaric level is given as

$$Z(p) = Z_1 + 0.5\,\frac{R}{g}\,(T_* + T_{SL})\,\log\left(\frac{P_G}{p}\right) \qquad (7.5)$$

where R is the gas constant for pure dry air, g the gravitational acceleration, Z_1 the height of the model's terrain, p_G the pressure at the surface of the earth, and p the value of the isobaric level. Basically, T_2 has been extrapolated downward at a lapse rate of 0.0065K per meter to define T_*, the ground temperature, and T_{SL}, the temperature at sea-level. If T_{SL} exceeds 290.66K and if T_* is less than or equal to 290.66, then T_{SL} is set equal to 290.66 in equation (7.5). If T_* exceeds 290.66, then T_{SL} is redefined as

$$T_{SL} = 290.66 - 0.005\ (T_* - 290.66)^2 \tag{7.6}$$

for use in (7.5).

7.3 The Deslosh Procedure

The isobaric height fields are subjected to a procedure known as "desloshing". The relative vorticity at 500 mb is computed from the wind components at that level, with m denoting the map factor.

$$\zeta = m^2 \left[\frac{\partial}{\partial x}\ (v/m) - \frac{\partial}{\partial y}\ (u/m)\right] \tag{7.7}$$

A stream function, ψ, is then obtained from the known values of vorticity by applying a relaxation procedure to the equation

$$\nabla^2\ \psi = \zeta \tag{7.8}$$

The stream function field is used in the inverse form of the balance equation to obtain Z^D_{500}, where the superscript D indicates that the height field has been desloshed. The original hydrostatic height field, Z^H_{500}, is subtracted from Z^D_{500} to obtain the value of the deslosh at each point.

$$D = Z^D_{500} - Z^H_{500} \tag{7.9}$$

The deslosh field is then added to each isobaric hydrostatic height to obtain the desloshed height field for that level

$$Z^D = Z^H + D \tag{7.10}$$

In equation (7.7) the relative vorticity, ζ, is computed only for interior points. On the boundary it is set to zero. A scaled value of Z^H_{500} is used as the boundary condition on ψ in (7.8), and in the inverse form of the balance equation Z^H_{500} is used as the boundary condition in obtaining Z^D_{500}. Essentially, the deslosh procedure preserves the value of Z^H on the boundary at all levels. It adjusts interior values of Z^D_{500} to fit the boundary values and the forecast 500 mb vorticity at interior points. Finally, it preserves the original thickness between the 500 mb level and all other isobaric levels.

7.4 The Filtering of the Forecast

After completion of the vertical interpolation from sigma to pressure and after the desloshing of the heights, all forecast fields are filtered on the LFM-II grid. A bilinear interpolation is then used to obtain values on the LFM-I grid. After interpolation to the LFM-I grid, most fields are again filtered. The only output quantities which are not filtered on the LFM-I grid are: precipitation amount, surface pressure, precipitable water, boundary layer potential temperature and wind components, tropopause temperature and wind components, and the vertical speed shear at the tropopause. It is the values on the LFM-I grid which are used as the official forecast.

8.1 Evaluation of the Circulation Forecasts

Tables 8.1.1 through 8.1.8 present monthly S1 scores for 500 mb height and sea-level-pressure forecasts from the LFM model for the period 1976 to 1979. The S1 scores were computed using a forty-nine point latitude-longitude grid centered over the United States. The gridpoint spacing is five degrees latitude by ten degrees longitude. The verifying analysis is the LFM analysis. All LFM forecasts were used in computing the results in the tables.

On 31 August 1977 LFM-II replaced LFM-I as the operational limited-area model. It is interesting to examine the tables of S1 scores to see whether the change of model is reflected there. It is our view that the S1 scores for the 500 mb height forecasts do not offer convincing evidence of change in the quality of the predictions at that level. However, the figures for the sea level pressure forecasts indicate an improved skill (lower S1 score) during the last two years. We believe that some of this change is due to the finer resolution of LFM-II. The improvement is evident at sea level but not at 500 mb because of the difference in scale of the circulation features at the two levels.

Table 8.1.9 contains S1 scores for the LFM 500 mb forecast heights for 1979 for separate western and eastern grids. The superiority of the eastern predictions over the western is clear. The western area forecasts are degraded more quickly because of the nearness of the upstream boundaries and the upstream sparse data area.

Table 8.1.1

S1 SCORES FOR 12-HOUR 500 MB FORECAST FROM

THE LFM MODEL

	1976	1977	1978	1979
Jan	16	17	18	17
Feb	16	17	19	17
Mar	16	18	17	19
Apr	21	18	20	18
May	20	20	25	21
Jun	22	23	22	20
Jul	23	21	22	24
Aug	22	20	21	22
Sep	21	21	21	20
Oct	18	19	18	20
Nov	16	18	17	18
Dec	15	18	16	18
Average	19	19	20	20

Table 8.1.2

S1 SCORES FOR 24-HOUR 500 MB FORECASTS FROM

THE LFM MODEL

	1976	1977	1978	1979
Jan	23	24	24	24
Feb	21	24	25	22
Mar	22	24	23	24
Apr	28	23	26	24
May	26	26	27	27
Jun	28	28	27	25
Jul	28	26	26	28
Aug	28	24	25	26
Sep	25	26	26	25
Oct	24	25	22	25
Nov	22	23	23	24
Dec	20	24	22	24
Average	25	25	25	25

Table 8.1.3

S1 SCORES FOR 36-HOUR 500 MB FORECASTS FROM

THE LFM MODEL

	1976	1977	1978	1979
Jan	31	32	32	31
Feb	28	31	32	28
Mar	29	30	30	31
Apr	36	29	33	31
May	35	33	35	34
Jun	36	35	32	31
Jul	35	32	32	34
Aug	35	31	31	32
Sep	33	33	33	31
Oct	31	31	28	31
Nov	29	30	29	30
Dec	27	31	29	31
Average	32	32	31	31

Table 8.1.4

S1 SCORES FOR 48-HOUR 500 MB FORECASTS FROM

THE LFM MODEL

	1976	1977	1978	1979
Jan		38	39	38
Feb	36	37	38	34
Mar	34	37	36	39
Apr	46	35	42	37
May	42	41	41	40
Jun	43	42	38	37
Jul	42	36	37	39
Aug	42	36	37	37
Sep	39	39	40	36
Oct	38	36	33	37
Nov	36	38	35	36
Dec	33	39	34	37
Average	39	38	38	37

Table 8.1.5

S1 SCORES FOR 12-HOUR SEA LEVEL PRESSURE FORECASTS

FROM THE LFM MODEL

	1976	1977	1978	1979
Jan	38	38	35	36
Feb	40	36	35	34
Mar	38	35	34	34
Apr	39	37	33	37
May	39	39	35	37
Jun	40	38	35	36
Jul	41	39	36	36
Aug	41	40	35	38
Sep	42	39	35	34
Oct	37	37	33	35
Nov	38	40	35	35
Dec	38	38	36	34
Average	39	38	35	35

Table 8.1.6

S1 SCORES FOR 24-HOUR SEA LEVEL PRESSURE FORECASTS

FROM THE LFM MODEL

	1976	1977	1978	1979
Jan	45	46	42	44
Feb	47	45	44	42
Mar	45	42	41	41
Apr	45	44	39	44
May	45	45	42	43
Jun	47	46	41	42
Jul	47	44	42	42
Aug	47	45	42	43
Sep	47	45	43	40
Oct	42	40	39	41
Nov	44	46	43	42
Dec	44	46	43	41
Average	45	45	42	42

Table 8.1.7

S1 SCORES FOR 36-HOUR SEA LEVEL PRESSURE FORECASTS

FROM THE LFM MODEL

	1976	1977	1978	1979
Jan	54	53	50	51
Feb	55	54	51	49
Mar	52	50	51	47
Apr	52	52	47	53
May	52	54	50	51
Jun	55	55	49	49
Jul	54	53	50	51
Aug	54	52	49	52
Sep	53	51	54	48
Oct	49	46	46	49
Nov	51	54	49	49
Dec	52	55	50	49
Average	53	52	50	50

Table 8.1.8

S1 SCORES FOR 48-HOUR SEA LEVEL PRESSURE FORECASTS

FROM THE LFM MODEL

	1976	1977	1978	1979
Jan		62	58	57
Feb	63	62	58	55
Mar	57	57	57	54
Apr	60	58	53	60
May	59	62	58	58
Jun	60	61	55	57
Jul	58	58	54	56
Aug	60	57	54	58
Sep	61	58	60	53
Oct	57	50	50	55
Nov	58	61	56	56
Dec	59	62	56	56
Average	59	59	56	56

Table 8.1.9

S1 SCORES FOR THE LFM-II 500 MB FORECASTS FOR THE YEAR 1979 OVER THE WESTERN (W) AND EASTERN (E) GRIDS. WEST IS THE AREA BETWEEN 105W AND 145W, 25N AND 55N. EAST IS THE AREA BETWEEN 65W AND 105W, 25N AND 55N.

	12-HR		24-HR		36-HR		48-HR	
	W	E	W	E	W	E	W	E
Jan	23	16	29	20	37	27	44	32
Feb	19	15	26	17	32	23	38	27
Mar	22	16	28	20	37	27	44	34
Apr	22	16	28	21	34	27	40	34
May	23	19	30	23	37	30	43	36
Jun	25	19	29	23	35	29	40	35
Jul	26	22	32	26	38	32	43	37
Aug	28	19	32	22	37	28	42	32
Sep	25	17	31	20	37	26	43	31
Oct	24	17	30	21	35	26	41	32
Nov	23	15	29	19	35	25	41	32
Dec	22	15	29	20	36	26	42	33
Average	24	17	30	21	36	27	42	33

8.2 Evaluation of the Precipitation Forecasts

Tables 8.2.1 and 8.2.2 present monthly results from the verification of the LFM precipitation forecasts. The figures are based on the occurrence of 0.01 inch of liquid precipitation in a twelve-hour period at members of a sixty station network located over the United States and southern Canada.

If the model predicts 0.01 inch or more in a given twelve-hour period and if 0.01 inch or more is observed at the reporting station, then this forecast is counted as correct. The threat score, TS, is computed as

$$TS = \frac{100\ C}{F + R - C} \qquad (8.2.1)$$

where C is the number of stations correct, F is the number forecast to have 0.01 inch or more and R is the number reporting at least that amount. The bias, B, is computed as

$$B = \frac{F}{R} \qquad (8.2.2)$$

and is a convenient measure of the tendency of the model to forecast too small or too large an area of significant precipitation.

Both tables 8.2.1 and 8.2.2 show a trend of improvement (higher threat scores) over the four-year period. As with the S1 scores for the sea-level pressure forecasts, we attribute some of this change to the introduction of LFM-II on the last day of August 1977. It is considered too early to judge the impact of the convective precipitation scheme introduced in June 1979.

Table 8.2.1

12-24 HOUR LFM PRECIPITATION FORECAST

BIAS (B) AND THREAT SCORE (TS)

	1976		1977		1978		1979	
	B	TS	B	TS	B	TS	B	TS
Jan	0.92	39	1.02	43	0.86	48	0.88	49
Feb	1.02	41	1.06	36	0.83	38	0.99	46
Mar	0.93	41	1.32	47	0.89	42	1.07	45
Apr	0.92	37	1.07	43	1.06	43	1.07	43
May	0.83	38	1.09	29	0.98	45	0.95	42
Jun	0.89	27	0.80	26	1.01	32	1.15	34
Jul	0.90	25	1.10	27	1.19	29	1.16	31
Aug	1.04	25	1.14	28	1.24	33	0.88	28
Sep	1.23	34	1.14	35	1.22	37	1.18	43
Oct	1.04	46	1.12	40	0.84	29	1.05	41
Nov	0.95	35	1.15	43	0.94	44	1.12	50
Dec	0.82	37	1.04	42	1.03	42	1.14	48
Average	0.96	35	1.09	37	1.01	39	1.05	42

Table 8.2.2

24-36 HOUR LFM PRECIPITATION FORECAST

BIAS (B) AND THREAT SCORE (TS)

	1976		1977		1978		1979	
	B	TS	B	TS	B	TS	B	TS
Jan	0.99	30	1.16	36	0.96	43	0.91	43
Feb	1.16	34	1.24	32	0.86	34	1.10	40
Mar	1.04	38	1.41	39	1.03	38	1.12	42
Apr	1.10	32	1.16	38	1.16	39	1.15	40
May	0.96	32	1.24	28	1.02	39	1.00	35
Jun	1.05	22	0.85	26	0.91	27	1.03	32
Jul	1.15	21	1.16	26	1.00	28	1.02	29
Aug	1.29	24	1.17	28	1.09	26	0.76	29
Sep	1.28	31	1.09	33	1.12	34	1.04	40
Oct	1.05	39	1.14	35	0.79	26	1.00	34
Nov	1.09	28	1.26	39	1.04	42	1.13	45
Dec	1.01	31	1.15	39	1.12	41	1.16	39
Average	1.10	30	1.17	33	1.01	35	1.04	37

REFERENCES

Brown, J. A. and K. A. Campana, 1978: An Economical Time-Differencing System for Numerical Weather Prediction. Monthly Weather Review, 106, 1125-1136.

Gerrity, J. P., 1977: The LFM Model--1976: A Documentation. NOAA Technical Memorandum NWS NMC 60.

Phillips, N. A., 1957: A Coordinate System Having Some Special Advantages for Numerical Forecasting. Journal of Meteorology, 14, 184-185.

Shuman, F. G., 1971: Resuscitation of an Integration Procedure. NMC Office Note 54, 55 pp.

(Continued from inside front cover)

NOAA Technical Memorandums

NWS NMC 49 A Study of Non-Linear Computational Instability for a Two-Dimensional Model. Paul D. Polger, February 1971, 22 pp. (COM-71-00246)

NWS NMC 50 Recent Research in Numerical Methods at the National Meteorological Center. Ronald D. McPherson, April 1971, 35 pp. (COM-71-00595)

NWS NMC 51 Updating Asynoptic Data for Use in Objective Analysis. Armand J. Desmarais, December 1972, 19 pp. (COM-73-10078)

NWS NMC 52 Toward Developing a Quality Control System for Rawinsonde Reports. Frederick G. Finger and Arthur R. Thomas, February 1973, 28 pp. (COM-73-10673)

NWS NMC 53 A Semi-Implicit Version of the Shuman-Hovermale Model. Joseph P. Gerrity, Jr., Ronald D. McPherson, and Stephen Scolnik, July 1973, 44 pp. (COM-73-11323)

NWS NMC 54 Status Report on a Semi-Implicit Version of the Shuman-Hovermale Model. Kenneth Campana, March 1974, 22 pp. (COM-74-11096/AS)

NWS NMC 55 An Evaluation of the National Meteorological Center's Experimental Boundary Layer model. Paul D. Polger, December 1974, 16 pp. (COM-75-10267/AS)

NWS NMC 56 Theoretical and Experimental Comparison of Selected Time Integration Methods Applied to Four-Dimensional Data Assimilation. Ronald D. McPherson and Robert E. Kistler, April 1975, 62 pp. (COM-75-10882/AS)

NWS NMC 57 A Test of the Impact of NOAA-2 VTPR Soundings on Operational Analyses and Forecasts. William D. Bonner, Paul L. Lemar, Robert J. Van Haaren, Armand J. Desmarais, and Hugh M. O'Neil, February 1976, 43 pp. (PB-256-075)

NWS NMC 58 Operational-Type Analyses Derived Without Radiosonde Data from NIMBUS 5 and NOAA 2 Temperature Soundings. William D. Bonner, Robert van Haaren, and Christopher M. Hayden, March 1976, 17 pp. (PB-256-099)

NWS NMC 59 Decomposition of a Wind Field on the Sphere. Clifford H. Dey and John A. Brown, Jr. April 1976, 13 pp. (PB-265-422)

NWS NMC 60 The LFM Model 1976: A Documentation. Joseph P. Gerrity, Jr., December 1977, 68 pp. (PB-279-419)

NWS NMC 61 Semi-Implicit Higher Order Version of the Shuman-Hovermale Model. Kenneth A. Campana, April 1978, 55 pp. (PB-286-012)

NWS NMC 62 Addition of Orography to the Semi-Implicit Version of the Shuman-Hovermale Model. Kenneth A. Campana, April 1978, 17 pp. (PB-286-009)

NWS NMC 63 Day-Night Differences in Radiosonde Observations in the Stratosphere and Troposphere. Raymond M. McInturff, Frederick G. Finger, Keith W. Johnson, and James D. Laver, September 1979, 54 pp. (PB80 117989)

NWS NMC 64 The Use of Drifting Buoy Data at NMC. David Wright, June 1980, 23 pp. (PB80 220791)

NWS NMC 65 Evaluation of TIROS-N Data, January-June 1979. David Wright, June 1980, 21 pp. (PB80 220494)

NOAA SCIENTIFIC AND TECHNICAL PUBLICATIONS

The National Oceanic and Atmospheric Administration was established as part of the Department of Commerce on October 3, 1970. The mission responsibilities of NOAA are to assess the socioeconomic impact of natural and technological changes in the environment and to monitor and predict the state of the solid Earth, the oceans and their living resources, the atmosphere, and the space environment of the Earth.

The major components of NOAA regularly produce various types of scientific and technical information in the following kinds of publications:

PROFESSIONAL PAPERS — Important definitive research results, major techniques, and special investigations.

CONTRACT AND GRANT REPORTS — Reports prepared by contractors or grantees under NOAA sponsorship.

ATLAS — Presentation of analyzed data generally in the form of maps showing distribution of rainfall, chemical and physical conditions of oceans and atmosphere, distribution of fishes and marine mammals, ionospheric conditions, etc.

TECHNICAL SERVICE PUBLICATIONS — Reports containing data, observations, instructions, etc. A partial listing includes data serials; prediction and outlook periodicals; technical manuals, training papers, planning reports, and information serials; and miscellaneous technical publications.

TECHNICAL REPORTS — Journal quality with extensive details, mathematical developments, or data listings.

TECHNICAL MEMORANDUMS — Reports of preliminary, partial, or negative research or technology results, interim instructions, and the like.

Information on availability of NOAA publications can be obtained from:

ENVIRONMENTAL SCIENCE INFORMATION CENTER (D822)
ENVIRONMENTAL DATA AND INFORMATION SERVICE
NATIONAL OCEANIC AND ATMOSPHERIC ADMINISTRATION
U.S. DEPARTMENT OF COMMERCE

6009 Executive Boulevard
Rockville, MD 20852

NOAA--S/T 81-121